

Analysis of Plasma Bubbles Observed in Night Airglow Emission Line OI 630.0 nm from Kolhapur Using All Sky Imager

A K. SHARMA¹, D. P. NADE^{*1}, S. S. NIKTE¹, R. N. GHODPAGE², P. T. PATIL²,
M. V. ROKADE¹ AND R. S. VHATKAR¹

¹Earth and Space Science Laboratory, Department of Physics, Shivaji University, Kolhapur, India- 416004

²Medium Frequency Radar, Indian Institute of Geomagnetism, Shivaji University Campus, Kolhapur, India-416004

^{*}dada.nade@gmail.com

ABSTRACT

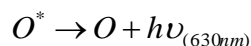
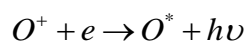
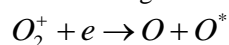
All-sky imager (ASI) located at Kolhapur (16.8° N, 74.2° E), India is used to observe OI 630.0 nm night airglow emission (at an altitude 250 km) during clear moonless nights. To study the characteristics of night airglow variations we have taken one month (February 2012) imager data of OI 630.0 nm emission line. The plasma bubbles have their own internal space-time dynamics [13] therefore result shows temporal variability in plasma motion. Due to change in the shape and size of plasma bubble some errors may occur in determination of the plasma velocity. So the reference of the western, eastern and middle wall/edge of the plasma bubble had been taken into account for calculating its velocity. The OI 630.0 nm emission having north-south aligned intensity depletion bands propagated from west to east with average velocity ~ 140 m/s. We found that the initially the plasma velocity is high and it decreases with time.

Keywords: *Night airglow, all sky imager, OI 630.0 nm emission line, Plasma bubble.*

1. INTRODUCTION

The variations in composition and structure of the ionosphere with latitude and altitude depend on the solar activities. The ionosphere has been widely studied using satellite and ground-based techniques. In the region between 80 to 300 km altitudes molecular/atomic emissions can be used to investigate and to sketch the airglow region circulation. The ground based measurements of various F-region and mesospheric nightglow emissions (OI 630 nm, 557.7 nm, 777.4 nm, Na (589.3 nm) and hydroxyl (OH) airglow) provide important information of the ionosphere-thermosphere during the different phases of a geomagnetic storm [5]. The studies of upper atmosphere of the Earth have been done using all sky imager with three different airglow emission lines (OI 630.0 nm, OI 557.7 nm, and OH) from Kolhapur (16.8°N, 74.2°E). At the equatorial F-region (at about 250-300 Km altitude) OI 630.0 nm night airglow emission line is used to investigate the thermosphere-ionosphere processes [9]. The low-latitude ionosphere bears the remarkable phenomena of plasma depletions or bubbles, which consist of extended regions of depleted F-region plasma [12]. The plasma bubble, a localized depletion in F-region electron density, is playing a major role in the equatorial spread-F phenomena [16]. Plasma is composed of an assembly of charged particles and is often referred to as the fourth state of matter because of its distinctive collective behavior while maintaining charge neutrality. Plasma bubbles are aligned along the magnetic flux tubes and cover north-south distances across the magnetic equator of several thousand kilometers, with east-west dimensions of up to a few hundred kilometers [11].

The F-region nightglow OI 630.0 nm emission line arising from [4, 6] dissociative and radiative recombination reactions as given below,



These chemical processes can be used to observe plasma bubbles, remotely and to study their development and dynamics [5]. The observed column of OI 630.0 nm emission intensity is proportional to the integral of the product of the O_2^+ , e (electron density) concentrations and charge transfer [11]. Several structures observed in the OI 630 nm airglow such as gravity wave signatures such as- brightness wave passage (which is linked to meridional winds driven by the midnight temperature maximum pressure bulge) and depletion patterns associated with equatorial spread F instabilities [3].

The wide-angle imaging of F-region nightglow emissions (e.g. OI 630 nm) arising from ionospheric recombination (dissociative and radiative) processes can be used to observe the onset, evolution and dynamics of plasma bubbles that comprise the envelope of spread-F irregularities [10]. To investigate the morphology of plasma bubble, it is necessary to develop an efficient image analysis method. All sky airglow images are not directly suitable for calculating the plasma velocity. Several methods are presented on image processing in the literature. The raw images were calibrated using the star background to determine the real azimuth on the image



[2]. Taylor and Garcia [15] reported method for analysis of wave signatures in the near-infrared OH and OI 557.7 nm emissions. The velocity of plasma bubble was determined by monitoring the position of plasma bubble in successive images, the east-west velocity [13] and north-south drift velocity [14].

2. ALL SKY IMAGER

All Sky Imager (ASI) (Make: Keo Scientific Ltd. Canada) has been installed by Indian Institute of Geomagnetism (I.I.G.), Navi Mumbai at Shivaji University Campus, Kolhapur. ASI is being used to observe the atmospheric airglow features or to study ionospheric irregularities. Fig. 1 shows the existent photo of the all-sky imager. All sky imager is framed in mainly three parts; Optical part consisting - fish eye lens (f/4 Mamiya RB67) with focal length 24 mm, a Telecentric optical lens combination and filter wheel. The fish eye lens, having 180° field of view, collects light from earth's atmosphere. The collected light beam is collimated by a telecentric optical lens combination. Then it passes through a narrow-band filter with nearly perpendicular incidence angles [1]. The six filters are installed in the filter wheel to allow the transmission of OI 630.0 nm, OI 557.7 nm, 840.0 nm, 846.0 nm, and OH Meinel bands at 720.0–910.0 nm and the transmission of background light at 857.0 nm. The second part of system is - detector, CCD camera (which is thermoelectrically cooled at a temperature of -80°C to reduce the thermal noise). After passing through the filter wheel, the collimated beam falls on CCD detector to make an image. The CCD (13.3×13.3 mm to 27.6×27.6 mm) detector is back-illuminated with an array of 1024×1024 pixels (quantum efficiencies greater than 95%) and 16 bits resolution. The CCD response is almost flat and differential gain of pixel is merely statistical in nature [8]. The last part of the system is an operating system. The filter wheel and camera shutter are controlled by a computer with the Windows XP operating system [7].



Fig. 1: Image of all sky imager

3. OBSERVATIONS AND RESULT

First we have taken the average of one hour raw data of image and then average image was subtracted from each raw image of one hour data. Due to this image processing, the plasma bubbles becomes clearly recognizable and their boundaries detectable in OI 630.0 nm. The difference between raw image and processed image is illustrated in Fig.2. In Fig 2, image (a) represents the actual OI 630.0 nm image in PNG format taken by all sky imager where nothing can be detectable, image (b) represents auto levels image created using Adobe Photoshop, image, here the signatures of plasma bubbles are observable (c) shows average image of one hour data taken from 160519 UT to 165702 UT (10 images with sampling rate about 6 min) and image (d) represents the mean image subtracted from raw image this image is the final where the good enhancement in the signatures of plasma bubbles are observable. For calculating plasma zonal velocity we traced the position of western wall, eastern wall and the center of plasma bubble in successive images. The references of western wall (b), eastern wall (c) and the center (d) of plasma bubble are illustrated in Fig 3.

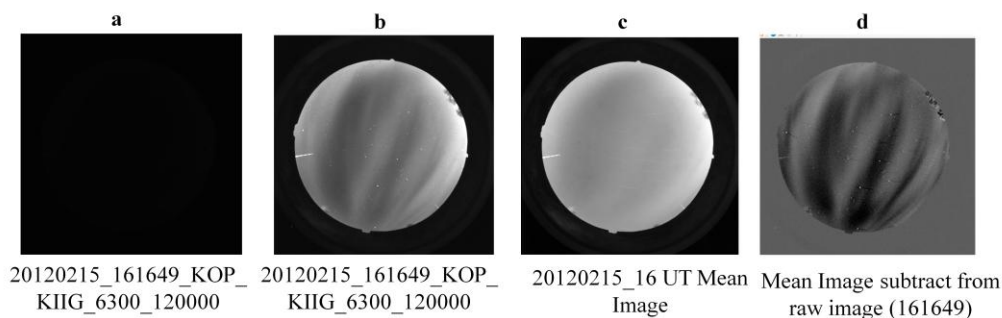


Fig. 2: Distinguish between raw image and processed image.

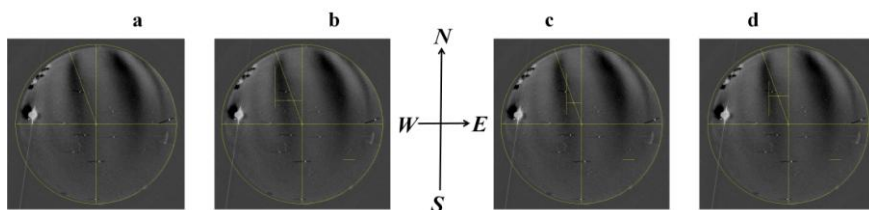


Fig. 3: (a) indicates that the image is divided into four quadrants with fixed center at (512, 512) pixel of image, (b) indicates the western wall of plasma bubble, (c) indicates the eastern wall of plasma bubble, and (d) indicates the center of plasma bubble.

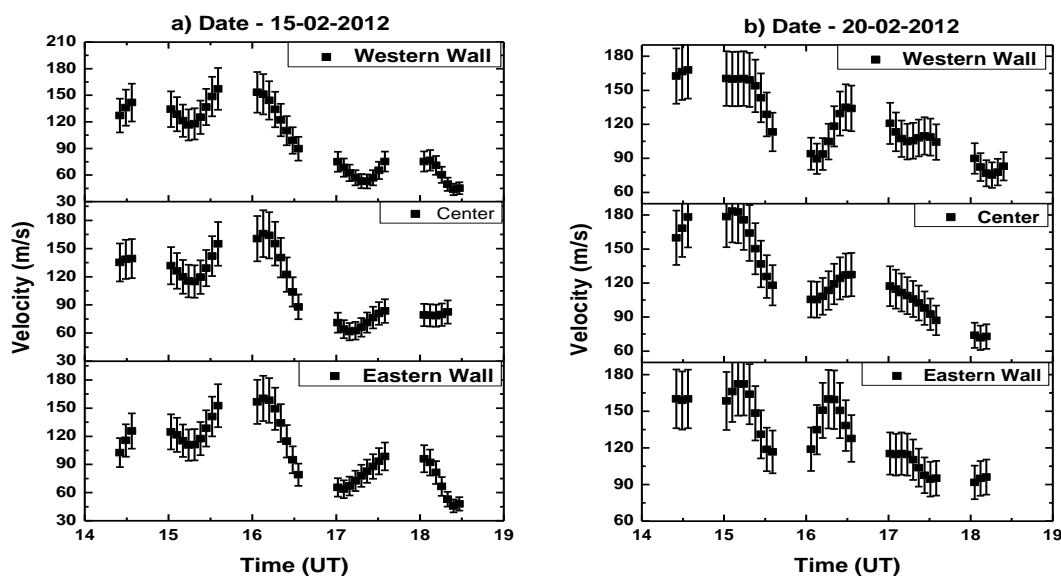


Fig. 4: Shows the plasma bubble velocity measured by monitoring the positions of its western wall, eastern wall and center.

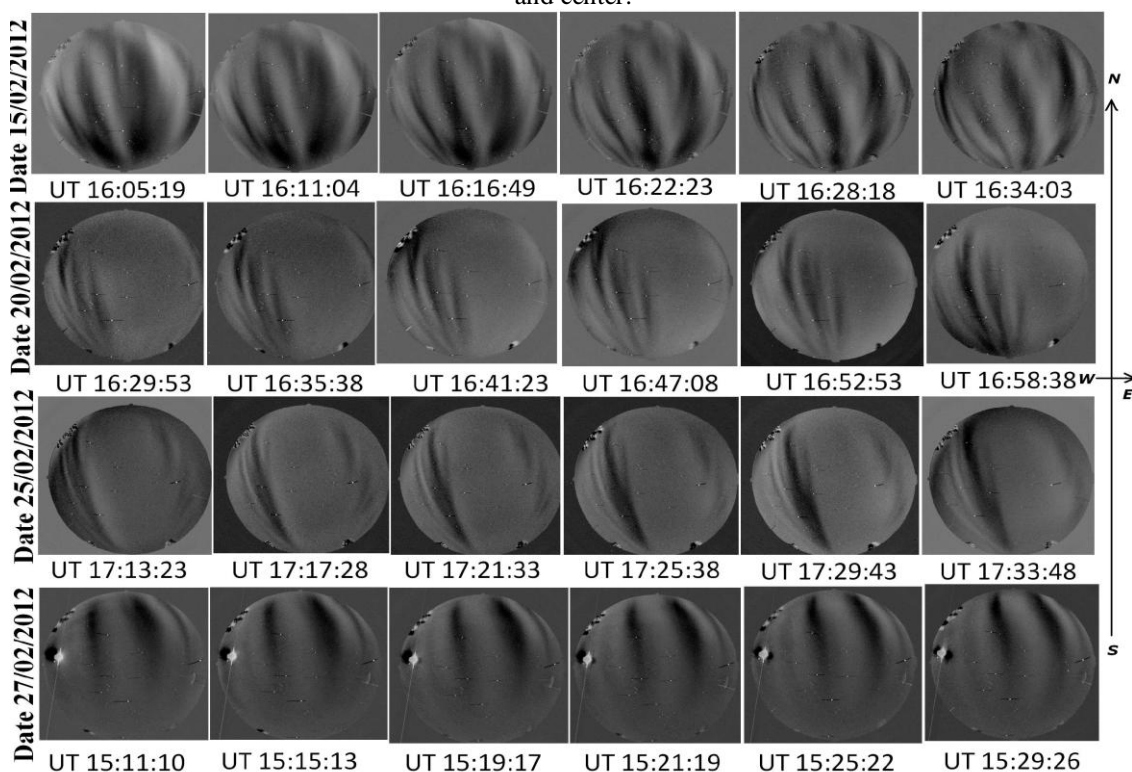


Fig. 5: Few sequences of images, OI 630.0 nm emission line, taken by all sky imager at Kolhapur during the nights of February 15, 20, 25 and 27, 2012

We have observed that the motion of eastern wall of plasma bubble is more stable than the western wall in many images while some images show in contrary. Therefore we have taken an average of motion of western wall; eastern wall and the center of plasma bubble to determine zonal velocity of plasma bubble. Fig 4a and 4b indicate plasma velocity on Feb. 15, 2012 and Feb. 20, 2012. From these figures it is clear that the western wall of the plasma was more stable than the eastern wall and middle of the plasma. There are data gaps in velocity plots due to non occurrence of plasma bubbles during the observation. Generally the plasma bubbles originate from south direction in the image and drifts from west to east.

We have taken image data of OI 630.0 nm night airglow emission, using all sky imager from Kolhapur during clear moonless night on Feb.2012. Fig. 5 illustrates few of the images of the OI 630 nm night airglow emission observed from Kolhapur on 15-16, 20-21, 25-26 and 27-28 February 2012 from 14 UT to 18 UT. By observing, the formation of plasma depletion, that occurred during midnight (at local time) and had taken about two hours to develop fully from west to east. However fully developed stage of plasma bubbles depend on local time variation of the vertical $E \times B$ plasma drift. In the present work, we have shown four days (out of 15 days) image data, because only for these days five hours event data is available. This five hour event (plasma bubbles) data is useful to find out the accuracy in plasma bubble drift velocity measurement by referring the western wall, eastern wall and the center plasma bubble.

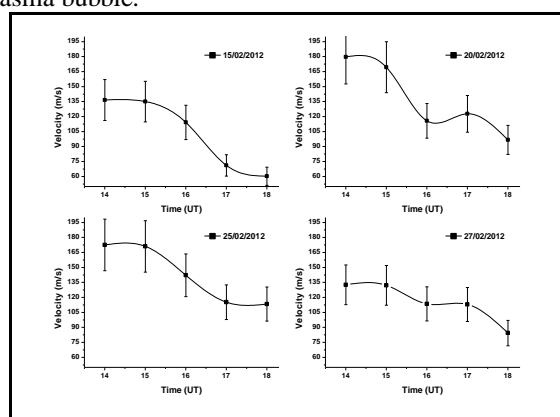


Fig. 5: The one hour average velocity of plasma bubble for Feb. 15, 20, 25 and 27, 2012.

We have calculated one hour average velocity of plasma bubble. Figure 6 shows the graphs of one hour average velocity of plasma bubble on 15-16, 20-21, 25-26 and 27-28 February 2012 from 14 UT to 18 UT. From Fig. 6 it is clear that the velocity of plasma bubble is high during the evening time and it goes on decreasing with time. The average error in the determination of the velocity ranged from 5 to 20 m/s. The average west-east velocity of the plasma was 140 m/s and it fluctuated between the velocity values from 60 m/s to 175 m/s. Generally plasma depletion has extended thousands of kilometers in north-south (magnetic equator) and in west-east hundreds of kilometers. The observed average width (extension of west-east direction) of plasma bubble was ~ 58 Km and it changed in the range between 40 km to 110 km. The north-south extension of the plasma depletion had average length of about 1164 km; the area of such size of a plasma bubble is about 304,800 km² at an altitude of 250 km.

The accuracy in the velocity measurement of plasma bubble also depends on its position on image. All sky images are curved and compressed at the low elevation angle because each pixel subtends an equal angle of the sky during formation of image onto the CCD. Thus two dimensional images are taken by all sky imager has curvature at edges. Due to this, the observed dimension of plasma bubbles varies with its position. At the middle of image, length and width of plasma bubble is greater than that of the edges. Thus the plasma bubbles occurring in middle area (up to 45° from the centre on the both sides) of the image are considered for the measurement plasma bubbles. From the above study it is observed that due to the sharp intensity gradient the plasma bubble drift velocity measured by using Eastern and Western wall is more accurate as compared to the middle of a plasma bubble.

4. DISCUSSION AND CONCLUSION

Plasma bubbles in OI 630.0 nm night airglow emission line have been observed with a new all sky imager system operating at Kolhapur in India. The image processing and its investigation has been done by using methods described in [3, 7], respectively. In the present work we have reported that the significant differences in the magnitude of plasma bubble velocities of its boundaries. The plasma bubbles have their own internal space-time dynamics [9] which changes the shape and size of bubble. To determine the velocity of plasma bubble, more accurately, we have taken average of velocities of western wall, eastern wall and center of plasma bubble. We have taken the average of velocity of western wall; eastern wall and center of bubble for calculating one hour average velocity. Observed propagation direction of plasma bubble was west to east which is in good



agreement with [10]. We observed that the plasma bubble required about two hours to develop fully. However, on an average, bubbles take about 2 hrs 35 min for the same [11]. The comparison of average zonal velocity (140 m/s) of plasma bubble agrees with previous study [10]. The average west-east velocity of plasma on 18-19 Feb. 1991 and on 20-21 Feb. 1991 were 150 m/s and 130 m/s respectively at same station [10]. The average velocity of north-south aligned plasma bubble was 140 m/s with west-east extension ~ 58 km. The average length of north-south aligned plasma depletion was 1164 km with area 304,800 km² at an altitude 250 km. Plasma velocity decreases with time since neutral wind intensities decrease was reported by P. M. Terra et al. [12]. The variation in motions of western wall and eastern wall of plasma bubbles depend on a local time of vertical $E \times B$ plasma drift. However the main mechanism for the generation of large scale structures associated with the spread F is the Generalized Rayleigh-Taylor Instability (GRTI) mechanism [11].

ACKNOWLEDGEMENTS

One of the authors Mr. D. P. Nade is thankful to DST-PURSE for research assistant. The nightglow observations at Kolhapur were carried out under scientific collaboration program between Shivaji University, Kolhapur and Indian Institute of Geomagnetism (I.I.G.), Navi Mumbai.

REFERENCES

- [1] Chung, J.-K., Y. H. Kim, Y.-I. Won B. Y. Lee (2003), Observation of Atmospheric Waves in the OH Airglow Layer with an All-Sky Camera, *Journal of the Korean Meteorological Society*, **39**, 3, pp 359-368.
- [2] Garcia, F. J., M. J. Taylor, M. C. Kelley (1997), Two-dimensional spectral analysis of mesospheric airglow image data, *Applied Optics*, **36**, pp 29.
- [3] Kubota, M., H. Fukunishi, S. Okano (2001), Characteristics of medium- and large-scale TIDs over Japan derived from OI 630-nm nightglow observation, *Earth Planets Space*, **53**, pp 741-751.
- [4] Mukherjee, G. K., L. Carlo, S. H. Mahajan (2000), 630 nm nightglow observations from 17° N latitude, *Earth Planets Space*, **52**, pp 105-110.
- [5] Mukherjee, G. K. (2006), Airglow and other F-layer variations in the Indian sector during the geomagnetic storm of February 5-7, 2000, *Earth Planets Space*, **58**, pp 623-632.
- [6] Mukherjee, G. K., D. J. Shetti (2008), Plasma drift motion in F-region of ionosphere using photometric nightglow measurements, *Indian Journal of Radio & Space Physics*, **37**, pp 249-257.
- [7] Mukherjee, G. K., Sikha R. Pragati, N. Parihar, R. Ghodpage, P. T. Patil, (2010), Studies of the wind filtering effect of gravity waves observed at Allahabad (25.45°N, 81.85°E) in India, *Earth Planets Space*, **62**, pp 309-318.
- [8] Narayanan, V. L., S. Gurubaran, K. Emperumal (2009), Imaging observations of upper mesospheric nightglow emissions from Tirunelveli (8.7°N), *Indian Journal of Radio & Space Physics*, **38**, pp 150-158.
- [9] Pimenta, A. A., J. A. Bittencourt, P. R. Fagundes, Y. Sahai, R. A. Buriti, H. Takahashi, M. J. Taylor (2003), Ionospheric plasma bubble zonal drifts over the tropical region: a study using OI 630 nm emission all-sky images, *Journal of Atmospheric and Solar-Terrestrial Physics*, **65**, pp 1117-1126.
- [10] Sahai, Y., P. R. Fagundes, J. A. Bittencourt (2000), Transequatorial F-region ionospheric plasma bubbles: solar cycle effects, *Journal of Atmospheric and Solar-Terrestrial Physics*, **62**, pp 1377-1383.
- [11] Sahai, Y., P. R. Fagundes, J. R. Abalde, A. A. Pimenta, J. A. Bittencourt, Y. Otsuka, V. H. Rios (2004), Generation of large-scale equatorial F-region plasma depletions during low range spread-F season, *Annales Geophysicae*, **22**, pp 15-23.
- [12] Terra, P. M., J. H. A. Sobral, M. A. Abdu, J. R. Souza, H. Takahashi (2004), Plasma bubble zonal velocity variations with solar activity in the Brazilian region, *Annales Geophysicae*, **22**, pp 3123-3128.
- [13] Pimenta A. A., P. R. Fagundes, J. A. Bittencourt, Y. Sahai, D. Gobbi, A. F. Medeiros, M. J. Taylor, H. Takahashi (2001), Ionospheric Plasma Bubble Zonal Drift: A Methodology Using OI 630 nm All-Sky Imaging System, *Adv. Space Res*, **27**, 6-7, pp 1219-1224.
- [14] Taylor M. J. (1997), A Review Of Advances In Imaging Techniques For Measuring Short Period Gravity Waves In The Mesosphere And Lower Thermosphere, *Adv. Space Res*, **19**, pp 7-616.
- [15] Taylor, M. J. and F. J. Garcia (1995), A Two-Dimensional Spectral Analysis Of Short Period Gravity Waves Imaged In The OI (557.7nm) And Near Infrared OH Nightglow Emissions Over Arecibo, *Puerto Rico, Geophys. Res. Lett.*, **22**, pp 2473.
- [16] Tsunoda R. T., R. C. Livingston, J. P. McClure and W. B. Hanson (1982), Equatorial Plasma Bubbles: Vertically Elongated Wedges from the Bottomside F Layer, *Journal of Geophysical Research*, **87** (A11): 10.1029/J0GREA000087000A11009171000001, ISSN: 0148-0227

